DOI: 10.1002/ejic.200600491

# Assembly and Upconversion Properties of Lanthanide Coordination Polymers Based on Hexanuclear Building Blocks with ($\mu_3$-OH) Bridges

**Danfeng Weng,[a] Xiangjun Zheng,*[a] and Linpei Jin*[a]**

**Keywords:** Hydroxido clusters / Lanthanide coordination polymers / Codoped complexes / Upconversion properties

Three novel hexanuclear core-based hydroxidolanthanide coordination polymers $[Ln_3(BDC)_{3.5}(OH)_2(H_2O)_2]\cdot H_2O$ [Ln = Y (**1**), Yb (**2**) and Er (**3**); BDC = 1,4-benzenedicarboxylate] were prepared by the hydrothermal method. The controlled hydrolysis of lanthanide ions led to an open hexanuclear cluster core. The hexanuclear core containing six ($\mu_3$-OH) bridged $Ln^{III}$ ions from two asymmetric units adopts a chair-like configuration. It behaves as a building block and is linked by the BDC ligands to form a 3D framework. The guest water molecules occupy the 1D channels in the structure. The upconversion spectra of the Y:Er-Yb codoped coordination polymers have been studied. The distinct upconversion emissions come from two-photon or three-photon excitation of Y:Er-Yb codoped coordination polymers and arise from $Er^{III}$ transitions of the type $^4F_{5/2}\rightarrow{}^4I_{15/2}$, $^2H_{11/2}\rightarrow{}^4I_{15/2}$, $^4S_{3/2}\rightarrow{}^4I_{15/2}$ and $^4F_{9/2}\rightarrow{}^4I_{15/2}$.


## Introduction

Polynuclear hydroxidolanthanide cluster compounds are enjoying increasing popularity due to their optical, electronic and catalytic properties, which may ultimately lead to potential technological applications such as optoelectronic devices, luminescent and biocatalyst materials.[1] Many polynuclear hydroxidolanthanide clusters have been reported in the past two decades. The reported structures show that the basic structural skeletons belong to two motifs, i.e. cubane-like clusters and square pyramids with the $[Ln_4(\mu_3\text{-}OH)_4]^{8+}$ cubane-like building block being regarded as a common structural motif in hydroxidolanthanide clusters.[1b,2] Many tetranuclear hydroxidolanthanide clusters have a cubane-like building block.[1a,b,c;2b;3] Two cubane-like units can be combined to a heptanuclear $[Ln_7(\mu_3\text{-}OH)_8]^{13+}$ cluster sharing one vertex.[4] Four or five vertex-sharing cubane-like cluster units centring around a halide anion template can be assembled to dodeca-[1a,1c] and pentadecanuclear clusters[1a,1c;5] with wheel structures. The pentanuclear square-pyramid unit appears to be another common structural motif in hydroxidolanthanide clusters.[1d,6] The $[Eu_5(\mu_4\text{-}OH)(\mu_3\text{-}OH)_4]^{10+}$ cluster has been reported[7] and the square-pyramidal $Ln_5$ unit can be considered as a building block for hexa-,[1a,1c;8] nona-[6a,9] and tetradecanuclear[1d,6b,10] clusters sharing their apexes or the square bases. To the best of our knowledge, the majority of hexanuclear $[Ln_6(\mu_6\text{-}O)(\mu_3\text{-}OH)_8]^{8+}$ skeletons are octahedral while the $[Ln_6(\mu_3\text{-}OH)_4]^{14+}$ chair-like core as building block has never been reported.

In the past decade, the upconversion of the infrared light into visible light has been extensively studied on various crystalline and amorphous materials for their potential applications in lasers,[11] optical devices, wave-guides, data storage devices, microfabrication,[12] biological labelling,[13] biosensors[14] and so on. The most frequently used upconversion ions are $Er^{III}$ or $Tm^{III}$ combined with $Yb^{III}$ as a sensitiser. Many different RE-doped (RE = rare earths) inorganic materials have been studied such as oxides,[15] silicates and phosphates,[16] oxyfluorides,[17] fluorides[18] and $NaYF_4$.[13b,14a,19] However, very few lanthanide-doped coordination compound materials have been achieved.[20] We report herein three new hexanuclear hydroxidolanthanide cluster coordination polymers $[Ln_3(BDC)_{3.5}(OH)_2(H_2O)_2]\cdot H_2O$ [Ln = Y (**1**), Yb (**2**), Er (**3**)] which are different from the reported motifs and the first examples with upconversion properties of the codoped lanthanide (Y, Er, Yb) coordination polymers.

## Results and Discussion

### Synthesis

The coordination polymers were obtained by hydrothermal synthesis. During the preparation, the pH of the reaction systems was adjusted by aqueous NaOH in the presence of NaAc to control the hydrolysis of the lanthanide ions. Then 1,4-benzenedicarboxylic acid was added to the resultant mixture.

### Structural Description

The single-crystal X-ray diffraction analysis revealed that compounds **1**, **2** and **3** are isomorphous and, consequently,

[a] Department of Chemistry, Beijing Normal University, Beijing 100875, P. R. China
Fax: +86-10-58802075
E-mail: lpjin@bnu.edu.cn

   

we will only describe the structure of **1** in detail. The asymmetric unit of **1** consists of a neutral trinuclear $[Y_3(BDC)_{3.5}(OH)_2(H_2O)_2]$ unit (Figure 1) and one lattice water molecule. The three $Y^{III}$ ions are all eight-coordinate but surrounded by different numbers of $\mu_3$-OH groups, coordinated $H_2O$ molecules and BDC anions. Around Y1, Y2 and Y3, there are five, five and four BDC ligands, respectively. For BDC, which adopts two coordination modes in the compound, the coordinated carboxyl units are divided into two types: bridging bidentate (I) and chelating/bridging tridentate (II) (Scheme 1). The hydroxy groups adopt a $\mu_3$-mode to bridge three $Y^{III}$ ions, while the water molecule only acts as a terminal ligand. Thus, the three $Y^{III}$ ions are coordinated in markedly different coordination environments (see Table 1). Selected bond lengths of **1** are listed in Table 2.

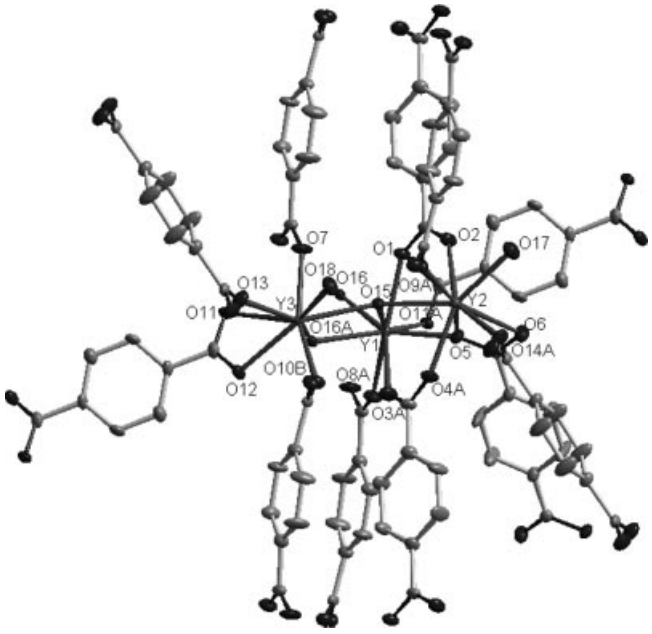


Figure 1. Coordination environment of $Y^{III}$ in complex **1** with ellipsoids drawn at the 30% probability level. All hydrogen atoms and lattice water molecule are omitted for clarity.

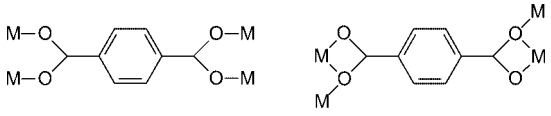


I II

Scheme 1. Coordination modes for the BDC ligands in **1**.

Table 1. The coordination environment of the $Y^{III}$ ions in the asymmetric unit.

| | No. of $\mu_3$-OH | No. of carboxylate oxygen atoms | | No. of $H_2O$ |
|---|---|---|---|---|
| | | I | II | |
| Y1 | 3 | 3 | 2 | 0 |
| Y2 | 1 | 3 | 3 | 1 |
| Y3 | 2 | 3 | 2 | 1 |

Table 2. Selected bond lengths in complex **1** [Å].

| | | |
|---|---|---|
| Y(1)–O(1) 2.362(2) | Y(2)–O(2) 2.336(2) | Y(3)–O(7) 2.226(2) |
| Y(1)–O(3)#1 2.408(2) | Y(2)–O(4)#1 2.335(2) | Y(3)–O(10)#1 2.231(2) |
| Y(1)–O(5) 2.263(2) | Y(2)–O(5) 2.436(2) | Y(3)–O(11) 2.821(2) |
| Y(1)–O(8)#2 2.293(2) | Y(2)–O(6) 2.500(3) | Y(3)–O(12) 2.414(2) |
| Y(1)–O(11)#2 2.431(2) | Y(2)–O(9)#3 2.254(2) | Y(3)–O(13) 2.235(3) |
| Y(1)–O(15) 2.388(2) | Y(2)–O(14)#4 2.300(2) | Y(3)–O(15) 2.479(2) |
| Y(1)–O(16) 2.412(2) | Y(2)–O(15) 2.429(2) | Y(3)–O(16)#2 2.315(2) |
| Y(1)–O(16)#2 2.278(2) | Y(2)–O(17) 2.363(3) | Y(3)–O(18) 2.394(3) |

Symmetry operations: #1: $x + 1, y, z$; #2: $-x + 1, -y + 1, -z + 1$; #3: $-x, -y + 2, -z + 1$; #4: $-x + 1, -y + 2, -z + 1$.

The three $Y^{III}$ ions combine with another three $Y^{III}$ ions from the adjacent asymmetric unit to form a second hexanuclear building block (Figure 2a). Every three adjacent $Y^{III}$ ions are linked by one $\mu_3$-OH group in the centre,

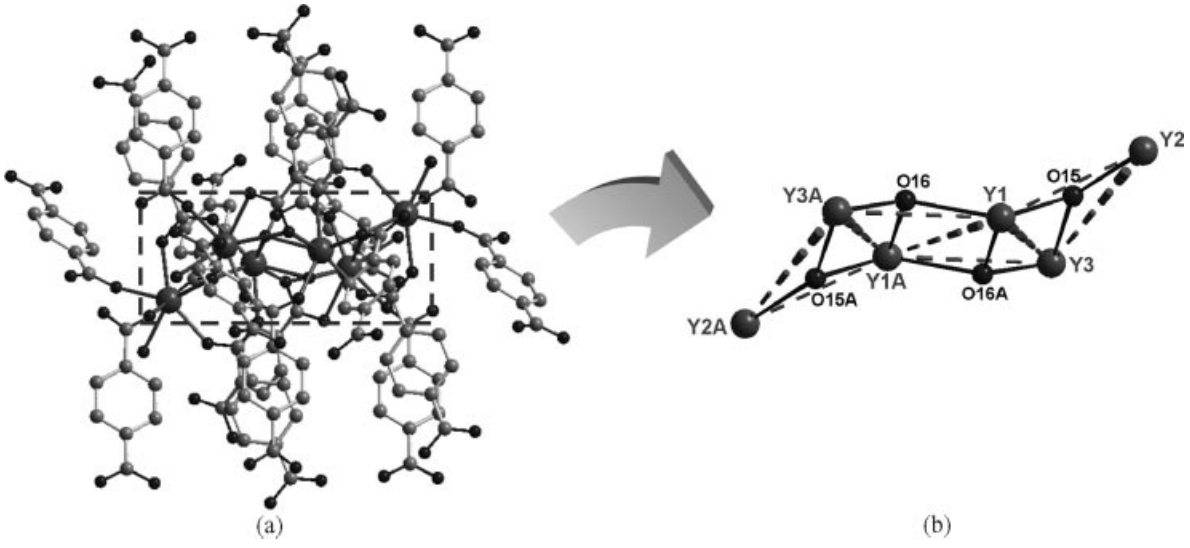


Figure 2. (a) Cell structure of **1**. (b) Chair-like conformation of the hexanuclear core.

  

which is slightly above the basal face and the Y–O($\mu_3$-OH) distances range from 2.278 to 2.479 Å. These distances are comparable with Ln–O($\mu_3$-OH) distances in the reported octahedral hexanuclear compounds with an average of 2.433 Å.[8d,8e] Four $Y_3$($\mu_3$-OH) trigonal pyramids share their adjacent sides to form the hexanuclear cluster with a chair-like conformation (Figure 2b). This chair-like hexanuclear building block is different from the reported structural motifs based on square pyramids and cubane-like cores. The Ln···Ln distances ranging from 3.731 to 4.712 Å are longer than those found in the latter two kinds of clusters (the majority range from 3.5 to 3.8 Å).[1b,3c,4,6,8d,8e,9] This is due to the steric effect of the open construction of the $Ln_6$ entity whereas the reported hexanuclear clusters are all closed clusters.

Among the reported hexanuclear hydroxido clusters, most were almost zero-dimensional.[8a,8b,8d,8e] One 1D example was achieved by linking the hydroxidolanthanide cluster through Pd ions[8c] and a reported pseudo-3D network is based on hydrogen bonds[8f] whereas the hexanuclear cores in the title compounds are linked by the ligand BDC, resulting in 3D coordination polymers. The BDC ligands act as short bridges through one carboxylato end linking the hexanuclear nodes or longer bridges through the two carboxylate groups. The linkages consist of ten BDC ligands along the *a*-axis, four along the [2 0 $\bar{1}$] direction, two along the [0 $\bar{1}$ 1] direction with the remaining two following the [$\bar{1}$ 1 0] direction. The linear rigid BDC ligands take the main role in linking the hexanuclear building blocks into a complicated 3D structure. The lattice water molecules, fixed by hydrogen-bonding interactions to the frameworks, are located in 1D channels in the 3D networks (see Figure 3).

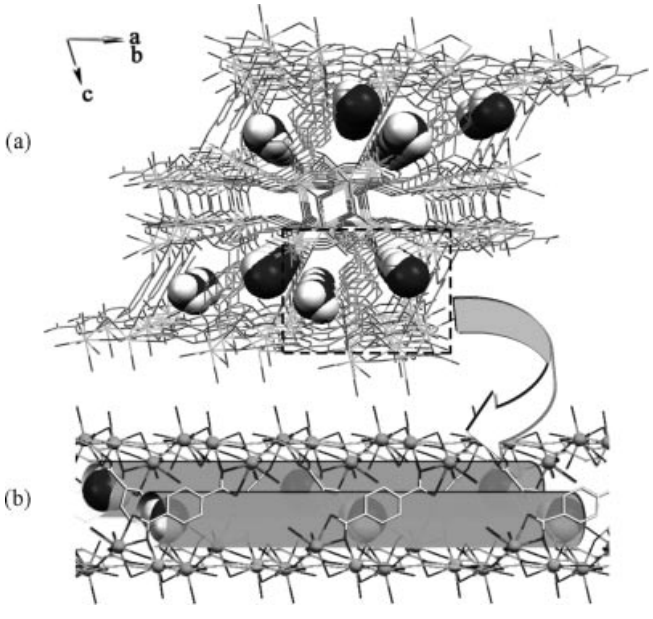


Figure 3. (a) Perspective view of the microporous framework of **1** along the [1 $\bar{1}$ 0] direction, showing 1D channels where guest water molecules reside and the guests are shown as space-filling models. (b) Lateral view of the 1D channels holding the water molecules.

## Upconversion Properties

The upconversion emission spectrum of the Y:Er-Yb codoped coordination polymer under 980 nm laser excitation is shown in Figure 4. The emission spectrum exhibits four bands. The red emission is centred at 654 nm and results from the $^4F_{9/2}(Er^{III})$ to $^4I_{15/2}(Er^{III})$ transition and the green band has centres at 545 and 524 nm and results from the transitions $^4S_{3/2}(Er^{III})/^2H_{11/2}(Er^{III})\rightarrow{}^4I_{15/2}(Er^{III})$. A seldom observed indigo emission centred at 455 nm can also be observed and corresponds to the transition $^4F_{5/2}(Er^{III})\rightarrow{}^4I_{15/2}(Er^{III})$.

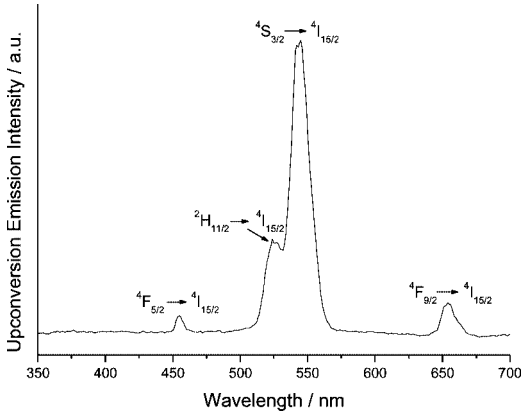


Figure 4. Upconversion emission for the $Er^{III}$ ion in the Y:Yb-Er codoped coordination polymer (laser power used is 640 mW, EM slit = 10.0 nm).

The 545 and 524 nm emissions can be described as a two-photon upconversion excitation mechanism.[15a,18a,18e,18f] First, the $Yb^{III}$ ions are easily excited to their $^2F_{5/2}(Yb^{III})$ level from ground $^2F_{7/2}(Yb^{III})$ level by absorbing a 980 nm photon. The energy is transferred to the $Er^{III}$ ions which become excited from the $^4I_{15/2}(Er^{III})$ level to the $^4I_{11/2}(Er^{III})$ level. A second photon transfer from the excited $Yb^{III}$ ions pumps the $Er^{III}(^4I_{11/2})$ ions to the $^4F_{7/2}(Er^{III})$ level. The $^4F_{7/2}(Er^{III})$ state can decay nonradiatively to the $^4S_{3/2}(Er^{III})$ and $^2H_{11/2}(Er^{III})$ levels.[15a,16c,18a] The green emissions observed result from the $^4S_{3/2}(Er^{III})\rightarrow{}^4I_{15/2}(Er^{III})$ and the $^2H_{11/2}(Er^{III})\rightarrow{}^4I_{15/2}(Er^{III})$ transitions. The decay processes were confirmed by a frequency of 2160 $cm^{-1}$ (1410 $cm^{-1}$ + 750 $cm^{-1}$, see Figure 5) and the peak at 1410 $cm^{-1}$ in the IR spectrum, for which the phonon energy corresponds to the energy gap between the $^4F_{7/2}(Er^{III})$ and $^4S_{3/2}(Er^{III})$ states, and the energy gap between $^4F_{7/2}(Er^{III})$ and $^2H_{11/2}(Er^{III})$ states. The possible channel for the green upconversion luminescence is given below:

$^2F_{5/2}(Yb^{III}) + {}^4I_{15/2}(Er^{III}) \rightarrow {}^2F_{7/2}(Yb^{III}) + {}^4I_{11/2}(Er^{III})$

$^2F_{5/2}(Yb^{III}) + {}^4I_{11/2}(Er^{III}) \rightarrow {}^2F_{7/2}(Yb^{III}) + {}^4F_{7/2}(Er^{III})$

$^4F_{7/2}(Er^{III}) \rightarrow {}^4S_{3/2}(Er^{III})/{}^2H_{11/2}(Er^{III})$ (nonradiative decay)

The 654 nm emission is caused by the transition to the $Er^{III}$ ground state $^4I_{15/2}(Er^{III})$ from the excited $^4F_{9/2}(Er^{III})$ state.[15a,18a,18e,18f] $Er^{III}$ ions in the $^4I_{11/2}(Er^{III})$ state lose their energy in the form of an OH vibration at 3500 $cm^{-1}$ [corresponding to the energy gap between $^4I_{11/2}(Er^{III})$ and $^4I_{13/2}(Er^{III})$], decay to the $^4I_{13/2}(Er^{III})$ state and then jump

  

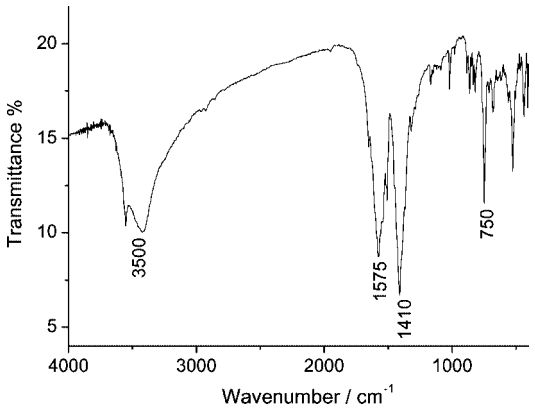


Figure 5. IR spectrum of the Y:Er-Yb codoped coordination polymer.

to the $^4F_{9/2}(Er^{III})$ level by a second pumping photon. This would account for the red emissions from the $^4F_{9/2}(Er^{III})$ level to the ground state. This mechanism can be described as:

$^2F_{5/2}\ (Yb^{III}) + {}^4I_{15/2}(Er^{III}) \rightarrow {}^2F_{7/2}(Yb^{III}) + {}^4I_{11/2}(Er^{III})$

$^4I_{11/2}(Er^{III}) \rightarrow {}^4I_{13/2}(Er^{III})$ (nonradiative decay)

$^2F_{5/2}\ (Yb^{III}) + {}^4I_{13/2}(Er^{III}) \rightarrow {}^2F_{7/2}(Yb^{III}) + {}^4F_{9/2}(Er^{III})$

The 455 nm indigo emission is unusual since upconversion emissions below 490 nm have seldom been observed for $Yb^{III}/Er^{III}$ materials.[15a] A probable three-photon mechanism for the population of the $^4F_{5/2}(Er^{III})$ level can be proposed to explain the indigo emission at 455 nm. There is a possibility that some excited $Er^{III}(^4I_{11/2})$ ions jump back to the lower $^4I_{13/2}(Er^{III})$ level giving the 3500 $cm^{-1}$ IR active decay. The two-photon energy from excited $Yb^{III}(^2F_{5/2})$ pumps the $Er^{III}(^4I_{13/2})$ to the $^2H_{9/2}(Er^{III})$ level via the $^2F_{9/2}(Er^{III})$ bridge and decays to the $^4F_{5/2}(Er^{III})$ level. The $^2H_{9/2}(Er^{III}) \rightarrow {}^4F_{5/2}(Er^{III})$ decay corresponds to 2325 $cm^{-1}$ (1575 $cm^{-1}$ + 750 $cm^{-1}$ in the IR spectrum). Therefore, the possible three-photon mechanism can be expressed as follows:

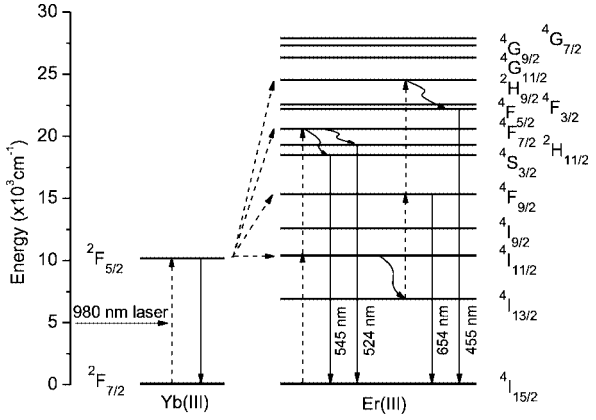


Figure 6. Energy-level diagram for the upconversion mechanism of the Y:Er-Yb codoped coordination polymer under 980 nm excitation.

$^2F_{5/2}\ (Yb^{III}) + {}^4I_{15/2}(Er^{III}) \rightarrow {}^2F_{7/2}(Yb^{III}) + {}^4I_{11/2}(Er^{III})$

$^4I_{11/2}(Er^{III}) \rightarrow {}^4I_{13/2}(Er^{III})$ (nonradiative decay)

$^2F_{5/2}\ (Yb^{III}) + {}^4I_{13/2}(Er^{III}) \rightarrow {}^2F_{7/2}(Yb^{III}) + {}^4F_{9/2}(Er^{III})$

$^2F_{5/2}\ (Yb^{III}) + {}^4F_{9/2}(Er^{III}) \rightarrow {}^2F_{7/2}(Yb^{III}) + {}^2H_{9/2}(Er^{III})$

$^2H_{9/2}(Er^{III}) \rightarrow {}^4F_{5/2}(Er^{III})$ (nonradiative decay)

The energy levels and overall upconversion Scheme of $Er^{III}$ are shown in Figure 6.

## Thermogravimetric Analysis and Powder X-ray Diffraction

We took complex **1** as a representative example for thermogravimetric analysis (see Figure 7). Under atmospheric conditions, thermogravimetric analysis performed on **1** showed the first weight loss of 5.5% in the range of 151–365 °C. This is related to the loss of the two coordinated water molecules and one lattice water molecule (calcd. weight loss 5.8%). The second mass loss began at 480 °C and is associated with the decomposition of the organic and hydroxy groups. The final residue, after the sample was heated to 836 °C, was $Y_2O_3$ (found weight loss 36.2%, calcd. 36.5%).

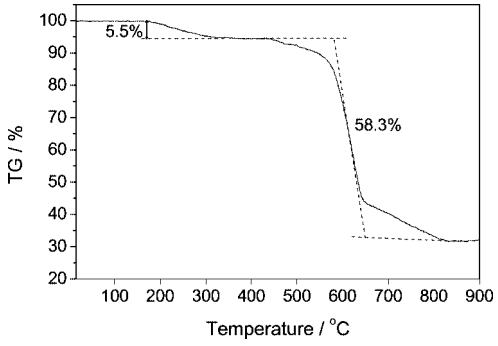


Figure 7. Thermogravimetric trace of **1**.

To confirm the thermogravimetric analysis, complex **1** was characterised by powder X-ray diffraction (PXRD) at 25, 100, 400, 635 and 880 °C (see Figure 8). The PXRD

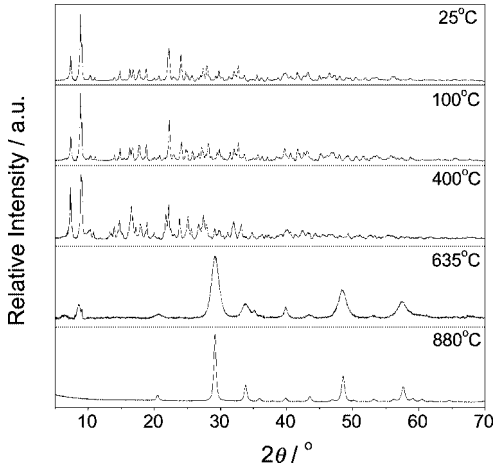


Figure 8. PXRD patterns for **1** taken at 25, 100, 400, 635 and 880 °C.

  

patterns of the sample at 100 and 400 °C, although very similar, are not the same, which indicates the change of the frameworks after the removal of the lattice water and coordinated water molecules. Above 635 °C, the PXRD patterns change completely, suggesting the collapse of the framework. The remaining residue $Y_2O_3$ coincides quite well with the standard $Y_2O_3$ (No. 01-083-0927).

## Conclusions

Three coordination polymers based on hexanuclear building blocks with ($\mu_3$-OH) bridges have been achieved. The hexanuclear building block has an interesting chair-like configuration which is different from the reported motifs based on cubane-like clusters and square pyramids. The structure of the cluster core depends on the extent of the hydrolysis of the Ln ions which is closely related to the pH of the system. Hence, controlled hydrolysis could lead to polymeric materials based on polynuclear clusters exhibiting different configurations. Furthermore, the Y:Er-Yb co-doped coordination polymers have been synthesised successfully. We have demonstrated the feasibility of introducing red, green and indigo light emissions of $Er^{III}$ ions using IR spectroscopy as supporting evidence for the nonradiative decay. The upconversion emissions of the codoped polymers correspond to two-photon and three-photon upconversion excitation mechanisms.

## Experimental Section

**General:** All chemicals were obtained commercially and used without further purification. Elemental analyses of C, H and N were performed with an Elementar Vario EL analyser. The IR spectra were recorded with a Nicolet Avatar 360 FTIR spectrometer using the KBr pellet technique. The thermal stability was investigated using a ZRY-2P thermogravimetric analyser under atmospheric conditions at a heating rate of 10 °C min$^{-1}$, using α-$Al_2O_3$ as a reference. The inductively coupled plasma (ICP) analysis was performed with a JY ULTIMA spectrometer. The powder X-ray diffraction was carried with a PANalytical X'Pert PRO MPD diffractometer using Cu-$K_{\alpha1}$ radiation in the $2\theta$ range of 5°–70°.

**Synthesis of $[Y_3(BDC)_{3.5}(OH)_2(H_2O)_2]\cdot H_2O$(1):** A solution of NaAc·3$H_2O$ (0.020 g, 0.15 mmol), $YCl_3\cdot 6H_2O$ (0.030 g, 0.1 mmol), $H_2O$ (5 mL) and aqueous NaOH (0.3 mL, 0.65 mol L$^{-1}$) was stirred to bring about the hydrolysis of $YCl_3$ and 1,4-benzenedicarboxylic acid (0.017 g, 0.1 mmol) was then added. The pH of the solution was adjusted to 5.1 and the mixture was then sealed in a 25 mL stainless steel reactor with a Teflon liner and heated at 190 °C for 72 h. Colourless block-like crystals of **1** were obtained. Yield: 0.021 g (66.67% based on Y). $C_{28}H_{22}O_{19}Y_3$ (929.19): calcd. C 36.19, H 2.39; found C 36.25, H 2.36. IR (KBr): $\tilde{\nu}$ = 553 (s), 3421 (s), 1651 (m), 1571 (s), 1540 (s), 1510 (m), 1410 (s), 1318 (w), 1169 (w), 1016 (m), 745 (s), 525 (m) cm$^{-1}$.

**Synthesis of $[Yb_3(BDC)_{3.5}(OH)_2(H_2O)_2]\cdot H_2O$(2):** This compound was prepared according to the procedure for **1** but by using $Yb(NO_3)_3\cdot 6H_2O$ instead of $YCl_3\cdot 6H_2O$. Diamond-like crystals of **2** were obtained. Yield: 0.020 g (49.61% based on Yb). $C_{28}H_{22}O_{19}Yb_3$ (1177.54): calcd. C 28.45, H 1.86; found C 28.50, H 2.01. IR (KBr): $\tilde{\nu}$ = 3555 (s), 3435 (s), 1654 (m), 1583 (s), 1539 (s), 1502 (m), 1408 (s), 1320 (w), 1170 (w), 1017 (m), 751 (s), 526 (m) cm$^{-1}$.

**Synthesis of $[Er_3(BDC)_{3.5}(OH)_2(H_2O)_2]\cdot H_2O$(3):** This compound was prepared according to the procedure for **1** but by using $ErCl_3\cdot 6H_2O$ instead of $YCl_3\cdot 6H_2O$. Pink diamond-like crystals of **3** were obtained. Yield: 0.016 g (41.47% based on Er). $C_{28}H_{22}O_{19}Er_3$ (1164.25): calcd. C 28.89, H 1.91; found C 29.08, H 1.89. IR (KBr): $\tilde{\nu}$ = 3550 (s), 3424 (s), 1650 (m), 1578 (s), 1538 (s), 1509 (m), 1408 (s), 1323 (w), 1174 (w), 1019 (m), 749 (s), 520 (m) cm$^{-1}$.

**Synthesis of $[(Y:Er\text{-}Yb)_3(BDC)_{3.5}(OH)_2(H_2O)_2]\cdot H_2O$:** The codoped compounds were prepared according to the procedure for **1** but by using $YCl_3\cdot 6H_2O$, $ErCl_3\cdot 6H_2O$ and $Yb(NO_3)_3\cdot 6H_2O$ (for example, molar ratio: 94.00:2.00:4.00%) instead of 100% $YCl_3\cdot 6H_2O$. Colourless block-like crystals were obtained. Yield: 0.018 g (56.88% based on total Ln). $C_{28}H_{22}O_{19}(Y:Er\text{-}Yb)_3$ (943.83): calcd. C 35.63, H 2.35; found C 35.85, H 2.43. IR (KBr): $\tilde{\nu}$ = 3554 (s), 3423 (s), 1653 (m), 1574 (s), 1535 (s), 1508 (m), 1410 (s), 1319 (w), 1167 (w), 1020 (w), 749 (s), 527 (m) cm$^{-1}$. The ICP analysis showed that the molar ratio of Y/Yb/Er was 94.45:2.17:3.38 in the product.

Table 3. Crystallographic data of **1**, **2** and **3**.

| | **1** | **2** | **3** |
|---|---|---|---|
| Empirical formula | $C_{28}H_{22}O_{19}Y_3$ | $C_{28}H_{22}O_{19}Yb_3$ | $C_{28}H_{24}O_{19}Er_3$ |
| Formula mass | 929.19 | 1177.54 | 1166.25 |
| $T$ [K] | 293(2) | 293(2) | 293(2) |
| Wavelength [Å] | 0.71073 | 0.71073 | 0.71073 |
| Crystal system | triclinic | triclinic | triclinic |
| Space group | $P\bar{1}$ | $P\bar{1}$ | $P\bar{1}$ |
| $a$ [Å] | 11.392(1) | 11.363(3) | 11.408(1) |
| $b$ [Å] | 12.070(1) | 11.989(3) | 12.064(1) |
| $c$ [Å] | 12.996(1) | 12.987(4) | 13.026(1) |
| $\alpha$ [°] | 86.898(1) | 86.741(4) | 86.827(1) |
| $\beta$ [°] | 67.176(1) | 67.084(4) | 67.126(1) |
| $\gamma$ [°] | 72.200(1) | 72.150(4) | 72.137(1) |
| $V$ [Å$^3$] | 1563.9(3) | 1547.1(7) | 1568.0(2) |
| Z | 2 | 2 | 2 |
| $D_c$ [g cm$^{-3}$] | 1.973 | 2.536 | 2.470 |
| $\mu$ [mm$^{-1}$] | 5.608 | 9.082 | 8.043 |
| Reflections collected, unique, $R_{int}$ | 10547, 7180, 0.0187 | 8207, 5447, 0.0336 | 8072, 5504, 0.0207 |
| $R$ indices [$I > 2\sigma(I)$] | $R_1$ = 0.0319, $wR_2$ = 0.0779 | $R_1$ = 0.0350, $wR_2$ = 0.0697 | $R_1$ = 0.0240, $wR_2$ = 0.0609 |
| $R$ indices (all data) | $R_1$ = 0.0457, $wR_2$ = 0.0886 | $R_1$ = 0.0492, $wR_2$ = 0.0749 | $R_1$ = 0.0267, $wR_2$ = 0.0621 |

  

The observed XRD patterns of the Y:Er-Yb codoped coordination polymer and **1** indicate that they are isomorphous.

**X-ray Structure Determination:** Intensity data for **1**, **2** and **3** were collected at 293 K with a Bruker SMART 1000 CCD area detector diffractometer using graphite-monochromated Mo-$K_\alpha$ radiation ($\lambda$ = 0.71073 Å) in $\varphi$ and $\omega$ scan modes with $\theta$ ranges of 1.78–27.88° for **1**, 2.09–25.01° for **2** and 1.70–25.01° for **3**. Semiempirical absorption corrections were applied using the SADABS program.[21] The structures were solved by direct methods[22] and refined by full-matrix least squares on $F^2$ using the SHELXS-97 and SHELXL-97 programs, respectively.[22,23] All non-hydrogen atoms were refined anisotropically. The hydrogen atoms were generated geometrically and treated with a mixture of independent and constrained refinements. Details of the crystallographic data of **1**, **2** and **3** are summarised in Table 3. CCDC-608985 to -608987 contain the supplementary crystallographic data for this paper. These data can be obtained free of charge from the Cambridge Crystallographic Data Centre via www.ccdc.cam.ac.uk/datarequest/cif.

**Luminescence Spectroscopy:** Upconversion spectra were obtained with an LS-50B fluorescence spectrophotometer (Perkin–Elmer Corp., Forster City, CA) with an external 0–800 mW adjustable laser (980 nm, Beijing Hi-Tech Optoelectronic Co., China) as the excitation source, instead of the xenon source in the spectrophotometer and with a fibre-optic accessory.

## Acknowledgments

We acknowledge the support from the National Natural Science Foundation of China (20331010, 20501003). We also thank Prof. Yadong Li from Department of Chemistry, Tsinghua University for help with the upconversion spectroscopic measurements.

[1] a) R. Y. Wang, H. D. Selby, H. Liu, M. D. Carducci, T. Z. Jin, Z. P. Zheng, J. W. Anthis, R. J. Staples, *Inorg. Chem.* **2002**, *41*, 278–286; b) B. Q. Ma, D. S. Zhang, S. Gao, T. Z. Jin, C. H. Yan, G. X. Xu, *Angew. Chem. Int. Ed.* **2000**, *39*, 3644–3646; c) Z. P. Zheng, *Chem. Commun.* **2001**, 2521–2529; d) M. R. Bürgstein, M. T. Gamer, P. W. Roesky, *J. Am. Chem. Soc.* **2004**, *126*, 5213–5218; e) O. Guillou, C. Daiguebonne, in: *Handbook on the Physics and Chemistry of Rare Earths*, Elsevier, Amsterdam, **2004**, vol. 34, p. 359–404.

[2] a) J.-C. G. Bünzli, C. Piguet, *Chem. Rev.* **2002**, *102*, 1897–1928; b) R. Y. Wang, H. Liu, M. D. Carducci, T. Z. Jin, C. Zheng, Z. P. Zheng, *Inorg. Chem.* **2001**, *40*, 2743–2750.

[3] a) J. C. Plakatouras, I. Baxter, M. B. Hursthouse, K. M. A. Malik, J. McAleese, S. R. Drake, *J. Chem. Soc., Chem. Commun.* **1994**, 2455–2456; b) T. Dube′, S. Gambarotta, G. Yap, *Organometallics* **1998**, *17*, 3967–3973; c) B. Q. Ma, D. S. Zhang, S. Gao, T. Z. Jin, C. H. Yan, *New J. Chem.* **2000**, *24*, 251–252; d) S. A. Schuetz, V. W. Day, J. L. Clark, J. A. Belot, *Inorg. Chem. Commun.* **2002**, *5*, 706–710; e) X. K. Fang, T. M. Anderson, C. Benelli, C. L. Hill, *Chem. Eur. J.* **2005**, *11*, 712–718.

[4] X. J. Zheng, L. P. Jin, S. Gao, *Inorg. Chem.* **2004**, *43*, 1600–1602.

[5] R. Y. Wang, Z. P. Zheng, T. Z. Jin, R. J. Staples, *Angew. Chem. Int. Ed.* **1999**, *38*, 1813–1815.

[6] a) G. Xu, Z. M. Wang, Z. He, Z. Lu, C. S. Liao, C. H. Yan, *Inorg. Chem.* **2002**, *41*, 6802–6807; b) R. Y. Wang, D. T. Song, S. N. Wang, *Chem. Commun.* **2002**, 368–369.

[7] R. G. Xiong, J. L. Zuo, Z. Yu, X. Z. You, W. Chen, *Inorg. Chem. Commun.* **1999**, *2*, 490–494.

[8] a) Z. Žák, P. Unfried, G. Giester, *J. Alloys Compd.* **1994**, *205*, 235–242; b) G. Giester, P. Unfried, Z. Žák, *J. Alloys Compd.* **1997**, *257*, 175–181; c) J. P. Liu, E. A. Meyers, S. G. Shore, *Inorg. Chem.* **1998**, *37*, 5410–5411; d) R. Y. Wang, M. D. Carducci, Z. P. Zheng, *Inorg. Chem.* **2000**, *39*, 1836–1837; e) D. S. Zhang, B. Q. Ma, T. Z. Jin, S. Gao, C. H. Yan, T. C. W. Mak, *New J. Chem.* **2000**, *24*, 61–62; f) N. Mahé, O. Guillou, C. Daiguebonne, Y. Gérault, A. Caneschi, C. Sangregorio, J. Y. Chane-Ching, P. E. Car, T. Roisnel, *Inorg. Chem.* **2005**, *44*, 7743–7750.

[9] L. G. Hubert-Pfalzgraf, N. Miele-Pajot, R. Papiernik, J. J. Vaissermann, *J. Chem. Soc., Dalton Trans.* **1999**, 4127–4130.

[10] M. R. Bürgstein, P. W. Roesky, *Angew. Chem. Int. Ed.* **2000**, *39*, 549–550.

[11] a) S. Sanders, R. G. Waarts, D. G. Mehuys, D. F. Welch, *Appl. Phys. Lett.* **1995**, *67*, 1815–1817; b) D. M. Baney, G. Rankin, K. W. Chang, *Appl. Phys. Lett.* **1996**, *69*, 1662–1664.

[12] a) F. Auzel, *Chem. Rev.* **2004**, *104*, 139–173; b) S. Q. Man, Y. B. E. Pun, P. S. Chung, *Appl. Phys. Lett.* **2000**, *77*, 483–485; c) R. Sivaraman, S. J. Clarson, B. K. Lee, A. J. Steckl, B. A. Reinhardt, *Appl. Phys. Lett.* **2000**, *77*, 328–330; d) D. R. Gamelin, H.-U. Güdel, *Acc. Chem. Res.* **2000**, *33*, 235–242.

[13] a) G. S. Yi, H. C. Lu, S. Y. Zhao, Y. Ge, W. J. Yang, D. P. Chen, L. H. Guo, *Nano Lett.* **2004**, *4*, 2191–2196; b) J. H. Zeng, J. Su, Z. H. Li, R. X. Yan, Y. D. Li, *Adv. Mater.* **2005**, *17*, 2119–2123.

[14] a) L. Y. Wang, R. X. Yan, Z. Y. Huo, L. Wang, J. H. Zeng, J. Bao, X. Wang, Q. Peng, Y. D. Li, *Angew. Chem. Int. Ed.* **2005**, *44*, 6054–6057; b) G. Piszczek, I. Gryczynski, B. P. Maliwal, J. R. Lakowicz, *J. Fluoresc.* **2002**, *12*, 15–17.

[15] a) J. Silver, M. I. Martinez-Rubio, T. G. Ireland, G. R. Fern, R. Withnall, *J. Phys. Chem. B* **2001**, *105*, 948–953; b) J. A. Capobianco, F. Vetrone, J. C. Boyer, A. Speghini, M. Bettinelli, *J. Phys. Chem. B* **2002**, *106*, 1181–1187; c) J. A. Capobianco, J. C. Boyer, F. Vertone, A. Speghini, M. Bettinelli, *Chem. Mater.* **2002**, *14*, 2915–2921; d) A. Patra, C. S. Friend, R. Kapoor, P. N. Prasad, *J. Phys. Chem. B* **2002**, *106*, 1909–1912; e) A. Patra, C. S. Friend, R. Kapoor, P. N. Prasad, *Appl. Phys. Lett.* **2003**, *83*, 284–286; f) H. W. Song, B. J. Su, T. Wang, S. Z. Lu, L. M. Yang, B. J. Chen, X. J. Wang, X. G. Kong, *Solid State Commun.* **2004**, *132*, 409–413; g) P. Salas, C. Angeles-Chávez, J. A. Montoya, E. De la Rosa, L. A. Diaz-Torres, H. Desirena, A. Martínez, M. A. Romero-Romo, J. Morales, *Opt. Mater.* **2005**, *27*, 1295–1300; h) C. Strohhöfer, A. Polman, *Opt. Mater.* **2003**, *21*, 705–712; i) G. S. Maciel, A. Biswas, P. N. Prasad, *Opt. Commun.* **2000**, *178*, 65–69.

[16] a) K. Riwotzki, H. Meyssamy, A. Kornowski, M. Haase, *J. Phys. Chem. B* **2000**, *104*, 2824–2828; b) K. Riwotzki, H. Meyssamy, H. Schnablegger, A. Kornowski, M. Haase, *Angew. Chem. Int. Ed.* **2001**, *40*, 573–576; c) F. Song, G. Y. Zhang, M. R. Shang, H. Tan, J. Yang, F. Z. Meng, *Appl. Phys. Lett.* **2001**, *79*, 1748–1750; d) G. A. Hebbink, J. W. Stouwdam, D. N. Reinhoudt, F. C. J. M. van Veggel, *Adv. Mater.* **2002**, *14*, 1147–1150; e) H. K. Jung, J. S. Oh, S. I. Seok, T. H. Lee, *J. Lumin.* **2005**, *114*, 307–313; f) S. Heer, O. Lehmann, M. Haase, H.-U. Güdel, *Angew. Chem. Int. Ed.* **2003**, *42*, 3179–3182.

[17] a) Y. H. Wang, J. Ohwaki, *Appl. Phys. Lett.* **1993**, *63*, 3268–3270; b) F. Lahoz, I. R. Martin, J. M. Calvilla-Quintero, *Appl. Phys. Lett.* **2005**, *86*, 051106; c) X. B. Chen, Z. F. Song, *Solid State Commun.* **2005**, *136*, 313–317.

[18] a) C. T. M. Ribeiro, A. R. Zanatta, L. A. O. Nunes, Y. Messaddeq, M. A. Aegerter, *J. Appl. Phys.* **1998**, *83*, 2256–2260; b) C. M. Bender, J. M. Burlitch, D. Barber, C. Pollock, *Chem. Mater.* **2000**, *12*, 1969–1976; c) J. W. Stouwdam, F. C. J. M. van Veggel, *Nano. Lett.* **2002**, *2*, 733–737; d) X. Wang, Y. D. Li, *Angew. Chem. Int. Ed.* **2003**, *42*, 3497–3500; e) R. X. Yan, Y. D. Li, *Adv. Funct. Mater.* **2005**, *15*, 763–770; f) S. Sivakumar, F. C. J. M. van Veggel, M. Raudsepp, *J. Am. Chem. Soc.* **2005**, *127*, 12464–12465.

[19] a) N. Menyuk, K. Dwight, J. W. Pierce, *Appl. Phys. Lett.* **1972**, *21*, 159–161; b) K. W. Krämer, D. Biner, G. Frei, H. U. Güdel, M. P. Hehlen, S. R. Lüthi, *Chem. Mater.* **2004**, *16*, 1244–1251.

[20] a) L. Luo, W. P. W. Lai, L. K. Wong, W. T. Wong, K. F. Li, K. W. Cheah, *Chem. Phys. Lett.* **2004**, *398*, 372–376; b) K.-L.

  

Wong, W. M. Kwok, W.-T. Wong, D. L. Phillips, K.-W. Cheah, *Angew. Chem. Int. Ed.* **2004**, *43*, 4659–4662.
[21] G. M. Sheldrick, *SADABS, Program for Empirical Absorption Correction of Area Detector Data*, University of Göttingen, Göttingen, Germany, **1997**.
[22] G. M. Sheldrick, *SHELXS 97, Program for Crystal Structure Solution*, University of Göttingen, Göttingen, Germany, **1997**.
[23] G. M. Sheldrick, *SHELXL 97, Program for Crystal Structure Refinement*, University of Göttingen, Göttingen, Germany, **1997**.

Received: May 27, 2006
Published Online: August 10, 2006

  